

A Photostable 1D Ruthenium–Zinc Coordination Polymer as a Multimetallic Building Block for Light Harvesting Systems

Seán Hennessey,^{*[a]} Christopher S. Burke,^[b] Roberto González-Gómez,^[a] Debobroto Sensharma,^[c] Wenming Tong,^[a] Amal,^[a] Cherian Kathalikkattil,^[c] Fabio Cucinotta,^[d] Wolfgang Schmitt,^[c] Tia E. Keyes,^[b] and Pau Farràs^{*[a]}

A luminescent ruthenium complex bearing two 2,6-di(quinolin-8-yl)-pyridine carboxylic acid (dqpCOOH) ligands has been successfully synthesised and fully characterised. The new metalloligand has been coordinated to zinc ions through the terminal carboxylate groups using a one-step solvothermal method, to give a multimetallic photoactive 1D coordination polymer, Ru–(dqpCOO)–Zn–(OOCH)₂. Through use of X-ray crystallography, advanced microscopy techniques as well as photophysical studies, we have extensively characterised the coordination polymer. The optical properties of the ruthenium

complex and corresponding coordination polymer show that the material experiences a dramatic increase in photostability compared to the free parent metalloligand, in solution. Electrochemical measurements of the coordination polymer also confirm the Ru^{II}/Ru^{III} redox couple is maintained in the polymeric network. The development of this material gives a new strategy in the design of novel photoactive materials as multimetallic building blocks for their use in light-based applications.

Introduction

Metal–organic frameworks (MOFs), a type of porous coordination polymer (PCP) formed by metal ions and organic linkers have gained widespread interest due to their porosity, tunability and high degrees of crystallinity and surface area.^[1–5] The variety of metal ions and organic linkers in these materials has led to diverse arrays of topologies and networks with applications in catalysis, inorganic conductors, gas storage and separation.^[6–8] Evolving from these promising materials is the design of structures with metalloligands replacing the organic linkers. These structures have a mixed-metal component, that

can alter both the architecture and chemical nature of the materials.^[9,10] Kumar and Gupta have shown in an extensive review, that the overall architecture, 1D/2D/3D, of metallopolymer networks and architectures can be highly controllable through rational and often facile approaches.^[11] In many cases the metalloligand can bind to the metal node through both carboxylate and amino terminal groups, much as that of PCPs and MOFs. This mixed-metal approach can lead to potentially interesting electrochemical and photophysical properties.^[12] Recent systems have used this strategy to create bimetallic materials with combinations such as Rh/Mn,^[13] Fe/Ag,^[14] Ru/Mn,^[15] and Ir/Nd.^[16] These mixed-metal combinations can be used to act as building blocks in the formation of 1D and 3D structures. The ruthenium systems are of particular interest, as ruthenium(II)-based molecular systems have shown great potential in the area of light harvesting, photocatalysis and artificial photosynthesis.^[17,18] Ruthenium containing mixed-metal networks, utilising Ru(bpy)₃²⁺ (bpy: 2,2'-bipyridine) moieties have been of particular impact due to their well understood photophysical properties.^[19–21] Similarly, Ru(tpy)₂²⁺ (tpy: 2,2';6',2''-terpyridine) complexes have been shown to form polymeric structures with applications in photoelectrochemistry and photocatalysis.^[22–24]

However, there are limitations to both Ru(bpy)₃²⁺ and Ru(tpy)₂²⁺ when applied as metalloligands. Ru(bpy)₃²⁺, although has both appropriate excited state redox potential and sufficiently long lived excited state to facilitate excited state electron transfer reactions,^[25] can form enantiomeric and diastereomeric mixtures. These mixtures prevent the ideal *trans* arrangement of donor and acceptor in the resulting polymer, leading to unfavourable back reactions.^[26] The Ru(tpy)₂²⁺

[a] S. Hennessey, Dr. R. González-Gómez, Dr. W. Tong, Dr. Amal, Dr. P. Farràs
School of Chemistry, Energy Research Centre, Ryan Institute,
National University of Ireland, Galway
Arts and Science Building, University Road, Galway (Ireland)
E-mail: s.hennessey1@nuigalway.ie
pau.farras@nuigalway.ie

[b] Dr. C. S. Burke, Prof. T. E. Keyes
School of Chemical Sciences, National Centre for Sensor Research,
Dublin City University, Dublin 9 (Ireland)

[c] Dr. D. Sensharma, C. Kathalikkattil, Prof. W. Schmitt
School of Chemistry, Trinity College Dublin
Chemistry Building, Dublin 2 (Ireland)

[d] Dr. F. Cucinotta
School of Natural and Environmental Sciences,
Newcastle University
Bedson Building 3.45, Newcastle upon Tyne, NE1 7RU (UK)

Supporting information for this article is available on the WWW under
<https://doi.org/10.1002/cptc.202100299>

© 2022 The Authors. ChemPhotoChem published by Wiley-VCH GmbH. This is an open access article under the terms of the Creative Commons Attribution Non-Commercial License, which permits use, distribution and reproduction in any medium, provided the original work is properly cited and is not used for commercial purposes.

complexes, despite providing a more ideal *trans* configuration, has much less useful excited-state lifetime of just 250 ps.^[27] Recent studies towards finding more promising ruthenium metalloligands have shown that the derivatives of the metal complexes of Ru(dqp)₂²⁺ (dqp: 2,6-di(quinolin-8-yl)-pyridine) hold promising properties.^[28–31] The Ru(dqp)₂²⁺ complexes have an excited-state lifetime in the μs time-scale, as well as comparable extinction coefficients and absorption profile in the visible region to Ru(bpy)₃²⁺ and Ru(tpy)₂²⁺ complexes. The dqp ligand also provides a larger bite angle than the Ru(tpy)₂²⁺ complexes, resulting in an increase in the ligand field splitting. The larger splitting leads to the usually rapid non-radiative decay seen in Ru(tpy)₂²⁺ complexes, resulting in a reduced emission lifetime.^[28]

Given these advantages, we have synthesised a novel 1D Ru–(dqpCOO)–Zn–(OOCH)₂ coordination polymer (RuZn polymer; empirical formula – C₅₀H₃₀N₆O₈RuZn) using a facile solvothermal method. This polymer is formed from the reaction between the newly synthesised metalloligand [Ru(dqpCOOH)₂](PF₆)₂ and zinc nitrate (see Figure 1). In addition, we have carried out a thorough structural and photophysical characterisation of the material.

Results and Discussion

The [Ru(dqpCOOH)₂](PF₆)₂ metal complex was synthesised via complexation between dqpCOOH and a previously synthesised Ru complex, *mer*-[Ru(dqpCOOEt)(CH₃CN)₃](PF₆)₂,^[32] and characterised by ¹H-NMR, MS and IR, the details of which are provided in the supporting information of this work (Figures S1–6). To synthesise the RuZn polymer, the ruthenium complex was treated as a typical linking ligand, as is seen in the synthesis of classical MOFs and PCPs, using Zn(NO₃)₂·6H₂O to provide the source of zinc ions. Formic acid was added in small quantities to act as a modulating unit in the development of a secondary building unit around the zinc ions.^[33] The decomposition of DMF, which was used as a solvent here, into formate groups has also been shown to aid in the formation of frameworks.^[34] As shown in Table S1, the optimised synthesis using a DMF:H₂O (85:15) mixture at 100 °C for 5 days produced red microcrystals of suitable quality for X-ray single crystal diffraction analyses, with the use of water as a solvent acting as a key component in the crystallisation of the polymer (Figure S6).

IR analysis of the dried crystalline product showed the representative bands of the free ruthenium complex still present (Figures S4 and S5), with a broad band appearing between 1590–1620 cm⁻¹. This is attributed to the formation of Zn–OOC bonds from either the zinc formate or through the carboxylate of the ruthenium complex. The band remaining at 1700 cm⁻¹ is assigned to the carboxylic acid terminal groups of the RuZn polymer. The thermal stability of the [Ru(dqpCOOH)₂](PF₆)₂ complex and RuZn polymer were analysed by thermal gravimetric analysis-differential scanning calorimetry (TGA-DSC), showing thermal stability in the RuZn polymer up to 300 °C (Figure S8). The 20% loss of weight between 50–160 °C is attributed to the residual DMF and H₂O present in the pores of the structure from the synthesis. The gradual reduction in weight after 300 °C is similar to that of the free ruthenium complex, suggesting break down of the linkage between the ruthenium and Zn components above this temperature.

The crystal structure of the polymer has also been resolved (Figures S9–S10 and Table S2), while selected bond lengths and angles present in the RuZn polymer are shown in Table S3. All the crystals that were examined were twinned alike. With the samples best suited for single-crystal analysis having to be cut to minimize rotational twin. As shown in Figure 2a, the polymer is formed through the carboxylate of the ruthenium complex binding to the zinc directly, and grows in a preferential 1D direction. This is unlike that of typical MOFs which classically develop metal nodes consisting of multi-metal clusters or the formation of secondary building units (SBUs).^[4] Here, the formic acid initially used as a modulating unit coordinates the Zn²⁺ cation to give a tetrahedral geometry as is seen in common zinc-based oxides and clusters.^[35] As a result of this, the total distance between the two ruthenium centres is 17.3 Å, while the distance between the two ruthenium centres in the adjacent chains of the polymer is 12.6 Å. The close proximity of the two ruthenium centres is encouraging for the further use of this material in light harvesting applications.^[36] Furthermore, this overlapping 1D network gives large unit cell volumes of 4.33 nm³ and a void volume of 0.51 nm³ (11.8% void space). This sizeable pore volume gives the hypothesis that the polymer should exhibit a degree of porosity. The crystal of the RuZn polymer also shows the adjacent chains have a moderate level of hydrogen bonding (Figure S11) between them, with a distance of 3.29 Å between the two formate groups bonded to the zinc cation. Effective hydrogen bonding through formate groups has been shown in previous MOFs and coordination

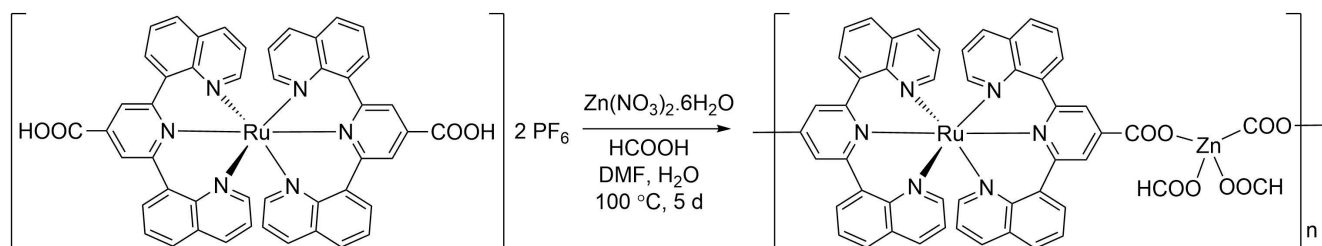


Figure 1. General synthesis conditions of conversion of [Ru(dqpCOOH)₂](PF₆)₂ complex to the RuZn polymer.

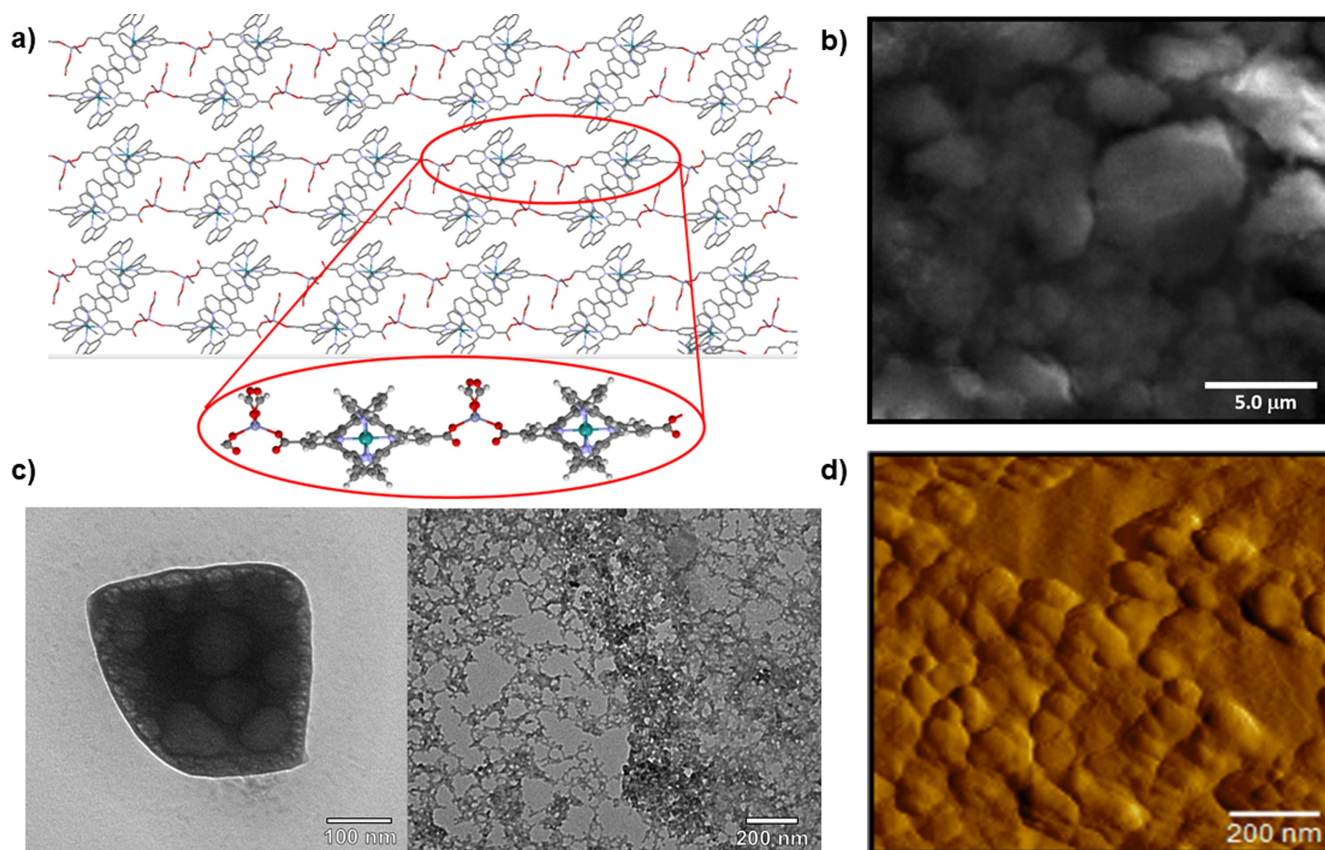


Figure 2. a) Expanded X-ray crystal structure of RuZn polymer, viewed along the *c*-axis. Inset: repeating structure of the RuZn polymer chain. Key: grey – carbon, white – hydrogen, red – oxygen, blue – nitrogen, green – ruthenium, purple – zinc. b) SEM image of the bulk RuZn polymer c) TEM images of the polymer (left – non exfoliated sample, right – exfoliated sample) d) AFM surface image of the bulk RuZn polymer.

polymers.^[37,38] The hydrogen bonding, coupled with the π - π interactions between the overlapping dq_p ligands of adjacent chains leads to improved stability in the RuZn polymer. Powder X-ray diffraction (PXRD) of the polymer was compared with the simulated XRD from the single crystal (Figure S12). As has been the case in other examples of zinc-containing coordination polymers, the simulated XRD does not fit well with experimental XRD as seen in other coordination polymers in the literature.^[39,40] This may be attributed to a range of factors, such as differences in the length of the 1D chains as a result of the poor solubility of the polymer at high temperatures in DMF, can lead to morphological differences.

Microscopy measurements were performed on the RuZn polymer for a better understanding of the morphology, shape and size of the material. Transmission electron microscopy (TEM) of a bulk sample of the polymer (Figure S13) show the formation of cuboidal grains of the material, grain size between 100–200 nm, with a porous-like appearance present in the material. When exfoliated, via ultrasonication at 50 °C for 6 h in a EtOH suspension (Figures 2c and S14), we observe in TEM the breakdown of these clusters into regular networks that display a repeating structure with a porous web-like shape. The web-like pattern forms through a system with an average width of 10.1 ± 0.2 nm (Figure S15), indicating that the network of the polymer is held together through several layers of the polymer.

Further to this, scanning electron microscopy-energy dispersive X-ray spectroscopy (SEM-EDX) was carried out on the bulk samples of the polymer to further clarify the morphology. The surface shown (Figures 2b, S16–S17) displays consistent cuboidal-like clusters of the polymer, as was shown in the bulk samples of the TEM, suggesting the polymer forms porous aggregates. Furthermore, the EDX measurements of the sample all consistently show the presence of both ruthenium and zinc (Tables S4–S5), confirming that the proportion of the two metal ions is present throughout the material. Atomic force microscopy (AFM) was also performed on the non-exfoliated RuZn polymer (Figure 2d and S18). Analysis of the mean size of the bulk polymer showed grains of 95.7 ± 66.8 nm in length, confirming the grain size of the bulk polymeric structure that was observed in TEM.

Cyclic voltammetry was performed to confirm the presence of the Ru^{II}/Ru^{III} redox couple is retained in the polymer. One reversible oxidation peak with $E_{1/2} = +1.22$ V for the free ruthenium complex in solution, consistent with typical Ru(II) polypyridyl complexes. With the polymer immobilised on FTO (via a Nafion solution due to the poor solubility in organic solvent), we observe a reversible redox process with an oxidation potential of $E_{1/2} = 1.25$ V (Figure S19), confirming the polymer still displays the same redox active capabilities of the free metalloligand, notwithstanding the necessarily different

experimental conditions that may affect the oxidation potential. The retention of redox activity is very promising for potential uses in photovoltaic and photocatalytic systems, as the redox centre is essential for these systems.^[41] Further to this, the RuZn polymer was immobilised directly onto a glassy carbon surface using Nafion, and its electrochemical stability examined (Figure S20). Over the course of 50 scans ($0 \rightarrow 1.6$ V), no observable breakdown of the polymer is observed after a UV-Vis measurement of the solvent. Additionally, we see no new bands appear in the cyclic voltammetry spectra, suggesting that, even under the strain of a high oxidation potential, the RuZn polymer is electrochemically stable. The slight drop in current observed during the experiment is attributed to passivation of the electrode or minor leaching of the material from the electrode surface, not observable in UV-Vis.

As $[\text{Ru}(\text{dqp})_2]^{2+}$ are known to show intense charge transfer transitions,^[42] UV-Vis absorption and emission spectroscopy studies on the polymer were carried out in comparison with the free ruthenium complex (Figure S21 and Table S6). Due to the poor solubility of the polymer in typical organic solvents, suspensions of the material were made in cyclohexane, which was found to yield the most homogeneous conditions to perform the measurements. The free ruthenium complex was measured in both acetonitrile and cyclohexane solutions, in order to ensure full comparison with the polymer; however, it should be noted that the solubility of the complex in cyclohexane is rather poor, which affects the definition of the optical profiles. The absorption spectrum of the polymer showed the typical features of Ru^{II} -polypyridyl complexes, with a broad MLCT band from 450 nm up to 600 nm and the intense $\pi-\pi^*$ transitions around 350 nm localised on the dqp ligand.

On the other hand, emission spectroscopy showed some interesting differences between the polymer and the parent Ru(II) complex. The latter displays a broad deep-red emission ranging from 650 to 850 nm, with a plateau at about 700 nm in acetonitrile, whereas two apparent peaks of equal intensity are observed in cyclohexane at 695 and 720 nm (Figures S22 and S23 respectively). Measurements carried out in deaerated solutions confirmed that the observed emission is due to phosphorescence from the $^3\text{MLCT}$ state, as the intensity increases nearly tenfold in absence of oxygen and the excited-state lifetime lengthens from 314 ns to about 2.55 ms (Figure S24 and Table S7). In contrast, the RuZn polymer shows multiple features in its emission spectrum (Figure 3), with a predominant, structured band at 540–555 nm and two bands of minor intensity at 690 and 755 nm, which recall the emission of the free ruthenium complex in solution. These bands could also suggest terminal groups of the polymer, with the semi-free ruthenium complex there displaying independent photoactive properties in comparison with the main polymeric chain, in the form of chain aggregation or mixed protonation at the termini. Alternatively, free ligand or dissociation of the metal complex from the chain could result in the formation of these bands. Significantly blue-shifted emission bands, although not as pronounced, have also been reported in other Zn(II)-based coordination polymers,^[43–45] whereby the rigidity imposed by the coordination to the organic ligands was found to be the

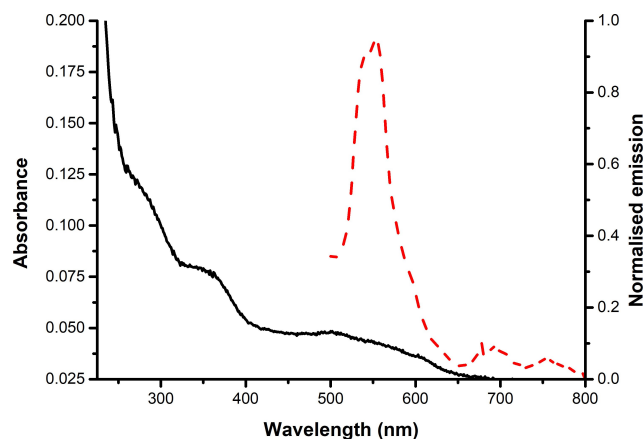


Figure 3. UV-vis (black solid) and emission spectra (red dashed) of RuZn polymer performed in a cyclohexane suspension, $\lambda_{\text{exc}} = 450$ nm.

main cause. The remarkable high-energy band could also indicate the emergence of a ligand-centred (LC) emission, localised on the dqp unit, which might prevail over the more common $^3\text{MLCT}$ emission as a result of changes in the localisation of the excitonic centres in the polymer and their interactions with the surroundings. In fact, the free dqpCOOH ligand in a cyclohexane suspension also shows an emission between 545–555 nm (Figure S25) giving further evidence to the hypothesis that LC emission is the prominent energy transition observed in the polymer.

The time-resolved analysis provided further insights, as it revealed that the high-energy emission is significantly more sensitive to oxygen than the deep-red emission (Table S7 and Figures S26–S27). The latter has a lifetime of 410 ns in absence of oxygen, and this is maintained in air-equilibrated conditions, the only difference being the appearance of a shorter-living component of 112 ns. On the other hand, the excited-state lifetime recorded at 540 nm decreases from 792 ns to less than 47 ns overall upon air-equilibration. This could point at a confirmation that different, decoupled excited states may exist in different regions of the polymer and that they would have a distinct sensitivity towards the solvent environment, for example terminal Ru(II)-based units vs. central units in the main polymeric chain. More detailed studies are currently ongoing in order to elucidate the full mechanism of luminescence and the structural factors controlling the exciton dynamics in the material.

Once the main emission properties were established, the photostability of the RuZn polymer was tested in comparison with the parent ruthenium complex. Steady irradiation was performed using the UV-visible light of a halogen flood lamp over the course of 24 h and the photoluminescence (PL) was monitored at regular intervals at 708 nm for $[\text{Ru}(\text{dqpCOOH})_2](\text{PF}_6)_2$ and 555 nm for the RuZn polymer (Figure 4, Figures S28–S29). After 2 h, the ruthenium complex displays over 50% reduction in PL intensity, which falls to 95% after 24 h. This may be due to ligand substitution reactions as reported previously for ruthenium polypyridyl complexes in acetonitrile under photoirradiation or photoisomerization to a

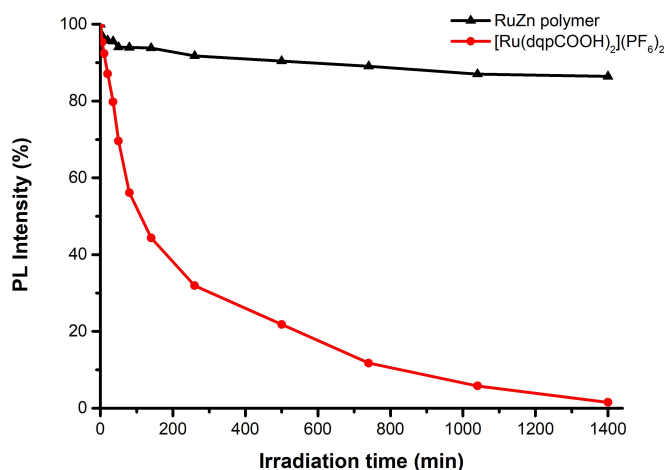


Figure 4. Photostability measurements based on PL intensity decrease over 24 h after light irradiation. RuZn polymer (black, triangles) performed in cyclohexane at $\lambda_{\text{exc}} = 480$ nm and PL measured at 550 nm. [Ru-(dqpCOOH)₂](PF₆)₂ (red, circles) performed in CH₃CN at $\lambda_{\text{exc}} = 480$ nm and PL measured at 708 nm.

non-emissive product. In contrast, the RuZn polymer in a cyclohexane suspension, exhibited a remarkable photostability, as only a 6% PL reduction was observed during the first 2 h of irradiation and about 84% of the initial PL intensity is maintained after 24 h. Further studies are underway to explore the mechanism involved in this significant increase in photostability, as well as the substantial blue-shift observed in the emission of the polymer.

Conclusion

In conclusion, we have synthesized a new, photoactive 1D RuZn coordination polymer, with distinctive improvements in the photostability of the RuZn polymer in comparison to its free Ru complex counterpart. This material also exhibits high thermal and chemical stability, as well as retaining the electrochemical properties of the free ruthenium complex. Furthermore, post synthetic modifications of these materials can be performed to transform the 1D nature of the material into 3D networks by alteration of the formate groups coordinated to the linking zinc atom. Overall, the formation of a stable, photoactive material through ruthenium metalloligands is promising for the creation of new structures for their use in light-harvesting, photocatalysis and photoelectrocatalysis.

Experimental Section

General experimental procedures for the synthesis of [Ru-(dqpCOOH)₂](PF₆)₂ and the RuZn polymer are described in the supporting information. The characterization data for these materials is also provided. Deposition Number 2123380 contains the supplementary crystallographic data for this paper. These data are provided free of charge by the joint Cambridge Crystallographic Data Centre and Fachinformationszentrum Karlsruhe Access Structures service.

Acknowledgements

S.H. acknowledges the College of Science at NUI Galway (NUIG) and the Royal Society of Chemistry for funding. W.T. and P.F. acknowledge the funding support from the INTERREG Atlantic Area programme under Grant Number EAPA_190/2016. R.G.G. acknowledge the funding from INTERREG Northern Periphery and Arctic programme under Grant Number 354. This publication has emanated from research conducted with the financial support of Science Foundation Ireland (SFI) under Grant Number 16/RI/3401 and 19/FFP/6428. The authors acknowledge the scientific and technical assistance of Dr. Éadaoin Timmins in the use of the AFM, SEM and TEM within the Centre for Microscopy & Imaging at NUIG, a facility that is funded by NUIG and the Irish Government's Programme for Research in Third Level Institutions, Cycles 4 and 5, National Development Plan 2007–2013, and Dr. Richard Bennett for advice in electrochemistry measurements. Open access funding provided by IReL.

Conflict of Interest

The authors declare no conflict of interest.

Data Availability Statement

The data that support the findings of this study are available in the supplementary material of this article.

Keywords: artificial photosynthesis · coordination polymers · light harvesting · metal–organic polymers · photostability

- [1] H. Li, M. Eddaoudi, M. O'Keeffe, O. M. Yaghi, *Nature* **1999**, *402*, 276–279.
- [2] O. M. Yaghi, M. O'Keeffe, N. W. Ockwig, H. K. Chae, M. Eddaoudi, J. Kim, *Nature* **2003**, *423*, 705–714.
- [3] S. Kitagawa, R. Kitaura, S. I. Noro, *Angew. Chem. Int. Ed.* **2004**, *43*, 2334–2375; *Angew. Chem.* **2004**, *116*, 2388–2430.
- [4] S. Batten, S. Neville, D. Turner, *Coordination Polymers*, Royal Society Of Chemistry, Cambridge, **2008**.
- [5] S. Bureekaew, S. Shimomura, S. Kitagawa, *Sci. Technol. Adv. Mater.* **2008**, *9*, 014108.
- [6] M. T. Nguyen, R. A. Jones, B. J. Holliday, *Coord. Chem. Rev.* **2018**, *377*, 237–258.
- [7] S. Noro, J. Mizutani, Y. Hijikata, R. Matsuda, H. Sato, S. Kitagawa, K. Sugimoto, Y. Inubushi, K. Kubo, T. Nakamura, *Nat. Commun.* **2015**, *6*, 5851.
- [8] J. Duan, W. Jin, R. Krishna, *Inorg. Chem.* **2015**, *54*, 4279–4284.
- [9] M. C. Das, S. Xiang, Z. Zhang, B. Chen, *Angew. Chem. Int. Ed.* **2011**, *50*, 10510–10520; *Angew. Chem.* **2011**, *123*, 10696–10707.
- [10] R. Horikoshi, T. Tominaga, T. Mochida, *Cryst. Growth Des.* **2018**, *18*, 5089–5098.
- [11] G. Kumar, R. Gupta, *Chem. Soc. Rev.* **2013**, *42*, 9403–9453.
- [12] S. Abednatanzi, P. Gohari Derakhshandeh, H. Depauw, F.-X. Coudert, H. Vrielandt, P. Van Der Voort, K. Leus, *Chem. Soc. Rev.* **2019**, *48*, 2535–2565.
- [13] C. T. Chapman, D. M. Ciurtin, M. D. Smith, H.-C. zur Loye, *Solid State Sci.* **2002**, *4*, 1187–1191.
- [14] L. Piñero-López, F. J. Valverde-Muñoz, M. Seredyuk, C. Bartual-Murgui, M. C. Muñoz, J. A. Real, *Eur. J. Inorg. Chem.* **2018**, *2018*, 289–296.
- [15] A. Dikhtiarenko, S. A. Khainakov, I. De Pedro, J. A. Blanco, J. R. Garcia, J. Gimeno, *Inorg. Chem.* **2013**, *52*, 3933–3941.
- [16] L. Li, S. Zhang, L. Xu, Z.-N. Chen, J. Luo, *J. Mater. Chem. C* **2014**, *2*, 1698.

- [17] Y. Kataoka, K. Sato, Y. Miyazaki, K. Masuda, H. Tanaka, S. Naito, W. Mori, *Energy Environ. Sci.* **2009**, *2*, 397–400.
- [18] A. Dikhtiarenko, P. Villanueva-Delgado, R. Valiente, J. García, J. Gimeno, *Polymer* **2016**, *8*, 48.
- [19] J. Lombard, D. A. Jose, C. E. Castillo, R. Pansu, J. Chauvin, A. Deronzier, M. N. Collomb, *J. Mater. Chem. C* **2014**, *2*, 9824–9835.
- [20] A. Kobayashi, T. Ohba, E. Saitoh, Y. Suzuki, S. Noro, H. Chang, M. Kato, *Inorg. Chem.* **2014**, *53*, 2910–2921.
- [21] A. Kuznetsova, V. Matveevskaya, D. Pavlov, A. Yakunenko, A. Potapov, *Materials (Basel)*. **2020**, *13*, 2699.
- [22] M. W. Cooke, P. M. Tremblay, G. S. Hanan, *Inorg. Chem. Commun.* **2007**, *10*, 1365–1370.
- [23] K. Feng, X. Shen, Y. Li, Y. He, D. Huang, Q. Peng, *Polym. Chem.* **2013**, *4*, 5701–5710.
- [24] T. Toyao, M. Saito, S. Dohshi, K. Mochizuki, M. Iwata, H. Higashimura, Y. Horiuchi, M. Matsuoka, *Chem. Commun.* **2014**, *50*, 6779.
- [25] B. Durham, J. V. Caspar, J. K. Nagle, T. J. Meyer, *J. Am. Chem. Soc.* **1982**, *104*, 4803–4810.
- [26] J. P. Sauvage, J. P. Collin, J. C. Chambron, S. Guillerez, C. Coudret, V. Balzani, F. Barigelletti, L. De Cola, L. Flamigni, *Chem. Rev.* **1994**, *94*, 993–1019.
- [27] J. R. Winkler, T. L. Netzel, C. Creutz, N. Sutin, *J. Am. Chem. Soc.* **1987**, *109*, 2381–2392.
- [28] M. Abrahamsson, M. Jäger, R. J. Kumar, T. Osterman, P. Persson, H.-C. Becker, O. Johansson, L. Hammarstrom, *J. Am. Chem. Soc.* **2008**, *130*, 15533–15542.
- [29] M. Jäger, R. J. Kumar, H. Görls, J. Bergquist, O. Johansson, *Inorg. Chem.* **2009**, *48*, 3228–3238.
- [30] C. Friebe, B. Schulze, H. Görls, M. Jäger, U. S. Schubert, *Chem. Eur. J.* **2014**, *20*, 2357–2366.
- [31] M. Majuran, G. Armendariz-Vidales, S. Carrara, M. A. Haghighatbin, L. Spiccia, P. J. Barnard, G. B. Deacon, C. F. Hogan, K. L. Tuck, *ChemPhotoChem* **2020**, *85*, 346–352.
- [32] M. Jäger, R. J. Kumar, H. Görls, J. Bergquist, O. Johansson, *Inorg. Chem.* **2009**, *48*, 3228–3238.
- [33] G. Wißmann, A. Schaate, S. Lilienthal, I. Bremer, A. M. Schneider, P. Behrens, *Microporous Mesoporous Mater.* **2012**, *152*, 64–70.
- [34] S. Quaresma, V. André, M. Martins, M. T. Duarte, *J. Chem. Crystallogr.* **2015**, *45*, 178–188.
- [35] D. Prochowicz, K. Sokolowski, J. Lewiński, *Coord. Chem. Rev.* **2014**, *270–271*, 112–126.
- [36] F. Fassioli, R. Dinshaw, P. C. Arpin, G. D. Scholes, *J. R. Soc. Interface* **2014**, *11*, 20130901.
- [37] G. Feng, D. Gui, W. Li, *Cryst. Growth Des.* **2018**, *18*, 4890–4895.
- [38] M. Sebghati, A. Tarahhomi, M. S. Bozorgvar, D. G. Dumitrescu, A. van der Lee, *RSC Adv.* **2021**, *11*, 8178–8197.
- [39] N. N. Adarsh, P. Dastidar, *Cryst. Growth Des.* **2011**, *11*, 328–336.
- [40] J. Hafizovic, M. Bjørgen, U. Olsbye, P. D. C. Dietzel, S. Bordiga, C. Prestipino, C. Lamberti, K. P. Lillerud, *J. Am. Chem. Soc.* **2007**, *129*, 3612–3620.
- [41] T. Koike, M. Akita, *Inorg. Chem. Front.* **2014**, *1*, 562–576.
- [42] M. Abrahamsson, H. C. Becker, L. Hammarström, *Dalton Trans.* **2017**, *46*, 13314–13321.
- [43] X. Xi, T. Dong, G. Li, Y. Cui, *Chem. Commun.* **2011**, *47*, 3831.
- [44] A. Gusev, E. Braga, Y. Baluda, M. Kiskin, M. Kryukova, N. Karaush-Karmazin, G. Baryshnikov, A. Kuklin, B. Minaev, H. Ågren, W. Linert, *Polyhedron* **2020**, *191*, 114768.
- [45] Y.-N. Wang, Y.-L. Ma, S.-S. Zhang, S.-F. Li, L. Du, Q.-H. Zhao, *Inorg. Chem. Commun.* **2021**, *126*, 108476.

Manuscript received: December 27, 2021
Accepted manuscript online: January 2, 2022
Version of record online: February 3, 2022